0026-895X/97/040542-09$3.00/0

MOLECULAR PHARMACOLOGY, **51**:542–550 (1997).

Overexpression of Glyceraldehyde-3-Phosphate Dehydrogenase Is Involved in Low K^+-Induced Apoptosis but Not Necrosis of Cultured Cerebellar Granule Cells

RYOICHI ISHITANI, KATSUYOSHI SUNAGA, MASAHARU TANAKA, HIDEKI AISHITA, and DE-MAW CHUANG

Group on Cellular Neurobiology, Josai University, Sakado, Saitama 350–02, Japan (R.I., K.S.), Fukui Research Institute, Ono Pharmaceutical Company, Ltd., Mikuni-cho, Fukui 913, Japan (M.T., H.A.), and Section on Molecular Neurobiology, Biological Psychiatry Branch, National Institute of Mental Health, National Institutes of Health, Bethesda, Maryland 20892 (D.-M.C.)

Received April 29, 1996; Accepted January 2, 1997

SUMMARY

We have reported that overexpression of glyceraldehyde-3-phosphate dehydrogenase (GAPDH; EC 1.2.1.12) is involved in age-induced apoptosis of the cultured cerebellar granule cells that grow in a depolarizing concentration (25 mM) of KCl. The present study was undertaken to investigate whether GAPDH overexpression also occurs and participates in apoptosis of the cerebellar granule cells that result from switching the culturing conditions from high (25 mM) to low (5 mM) concentrations of KCl. We found that exposure of granule cells to low potassium (K^+) for 24 hr induces not only apoptosis but also necrotic damage. The latter is supported by the morphological observations that a subpopulation of neurons showed cell swelling, extensive cytoplasmic vacuolization, damaged mitochondria, and apparently intact nuclei. Treatments with two antisense but not sense oligodeoxyribonucleotides directed against GAPDH attenuated low K^+-induced neuronal death by approximately 50%. Morphological inspection revealed that GAPDH antisense oligonucleotides preferentially blocked low K^+-induced apoptosis with little or no effect on necrotic damage. Similar to antisense oligonucleotides, actinomycin-D partially inhibited low K^+-induced death of granule cells with a predominant effect on apoptosis. In contrast, cycloheximide almost completely blocked low K^+-induced neuronal death and seemed to prevent both apoptotic and necrotic damage. The levels of GAPDH mRNA and protein were markedly increased in a time-dependent manner after low K^+ exposure. The overexpression of GAPDH mRNA and protein was completely blocked by cycloheximide, actinomycin-D, and its antisense but not sense oligonucleotides. Taken together, these results lend credence to the view that exposure of cerebellar granule cells to low K^+ induces both apoptosis and necrosis and that only the apoptotic component involves overexpression of GAPDH.

In the rat, CGC arise in the external germinal layer of the cerebellum shortly after birth. The cell bodies then migrate through the molecular layer to settle in the granule layer, but they leave behind their extended axons (1, 2). In the granule layer, the granule cells form short dendrites and receive glutamatergic innervations via mossy fibers. The granule cells project their axons, termed parallel fibers, to innervate the dendrites of other cerebellar neurons, such as Purkinje cells. The granule cell-to-Purkinje cell ratio is highly regulated and is thought to be maintained by neuronal apoptosis (3, 4). Because CGC differentiate after birth, they can be readily cultured from newborn rodents, and such primary cultures provide the most highly enriched *in vitro* system for the study of a single neuronal cell type. CGC in culture differentiate and mature into glutamatergic neurons capable of synthesizing and releasing glutamate (5). These processes require the presence of a depolarizing concentration of KCl or an initial activation of NMDA receptors (5, 6), which indicates an essential role of intracellular calcium. It has been reported that when mature CGC grown in high KCl are switched to a lower but more physiological concentration of KCl (i.e., 5 mM), they undergo cell death with morphological and biochemical hallmarks characteristic of apoptosis, including condensation and aggregation of chromatin, internucleosomal cleavage, and requirements for *de novo* RNA and protein synthesis (7, 8). This low K^+ switch-induced apoptosis of CGC can be protected by treatment with various excitatory amino acids (8) or insulin-like growth factor (7). However, the molecular mechanisms underlying this low K^+-induced apoptosis remain largely unknown.

We have recently reported that, under typical growth conditions (i.e., in the presence of 25 mM KCl without medium change and periodic glucose supplement), CGC spontaneously die by an apoptotic mechanism as the age of the cul-

ABBREVIATIONS: CGC, cerebellar granule cells; GAPDH, glyceraldehyde-3-phosphate dehydrogenase; NMDA, *N*-methyl-D-aspartate; FDA, fluorescein diacetate; PI, propidium iodide; PBS, phosphate buffered saline; CHX, cycloheximide; Act-D, actinomycin-D; ATA, aurintricarboxylic acid; SDS, sodium dodecyl sulfate; PAGE, polyacrylamide gel electrophoresis; THA, 9-amino-1,2,3,4-tetrahydroacridine; DIV, days *in vitro*.

tures reaches a critical stage, a process defined as age-induced apoptosis (9). This age-induced apoptosis of CGC is strikingly associated with overexpression of a 38-kDa protein in the particulate fraction, which has been identified as GAPDH (9). Antisense but not sense oligodeoxyribonucleotides to GAPDH protect against age-induced apoptosis of CGC. Moreover, GAPDH antisense oligonucleotides and other neuroprotectants suppress the age-induced accumulation of GAPDH mRNA and protein (9, 10). By the same criteria, GAPDH overexpression has been implicated in age-induced apoptosis of cultured cerebrocortical neurons (11) and cytosine arabinoside-induced apoptosis of cultured CGC (12). The present study was undertaken to further characterize low K^+-induced apoptosis, and, more importantly, to explore whether GAPDH also participates in this form of cell death. We present evidence that low K^+-induced CGC death involves multiple processes, including apoptosis, which involves GAPDH overexpression, and possibly necrosis, which does not. Some of these results have appeared as an abstract (13).

Experimental Procedures

Preparation of rat cerebellar neurons. CGC were prepared from 8-day-old Sprague-Dawley rat pups as previously described (5). Briefly, neurons were dissociated from carefully dissected cerebella by mechanical disruption in the presence of trypsin (0.025%) and DNase (0.008%) and were then plated in poly-L-lysine-coated 35-mm culture dishes. Cells were seeded at a density of 0.85–1.0 $\times$ 10^6 cells/ml (2 ml/dish) in basal modified Eagle's medium containing 10% fetal bovine serum and 25 mM KCl. Cytosine arabinoside (10 μM) was added to the culture medium 20 hr after plating to arrest the growth of non-neuronal cells. After 7–8 DIV, low K^+-induced apoptosis of CGC was carried out as described by D'Mello *et al.* (7). Cells were washed twice with and maintained in serum-free basal modified Eagle's medium (normally containing 5 mM KCl) supplemented with glutamine, gentamicin, and cytosine arabinoside in the absence or presence of test agents, as indicated elsewhere. For routine studies, cell viability was determined 24 hr after exposure to low K^+ concentrations.

Assessment of neuronal viability. Cells were washed with Locke's solution and double-stained with 0.0008% FDA, which is cleaved by esterases present in live cells, yielding yellowish-green fluorescein, and 0.0002% PI, which passes through the plasma membranes of dead cells to bind to DNA, producing orange-red nuclei (14). Both types of fluorescent cells can be simultaneously observed in a standard fluorescence microscope (Olympus IMT-2; Olympus, Tokyo, Japan). Cell viability was measured by the ratio of the number of FDA/FDA+PI positively stained cells in the photomicrographs of four representative squares (500 $\times$ 500 μm containing approximately 330 total cells) from each dish in a blind experiment.

Morphological examinations. Neurons grown in 35-mm plastic dishes were prefixed and postfixed in 3% glutaraldehyde and 1% OsO_4, respectively, dehydrated in ethanol, and embedded in Quetol 812 (Nisshin EM, Tokyo, Japan) for electron microscopy. *In situ* embedding of cultures, preparation of ultrathin sections, and double electron staining of those specimens were performed as described previously (9). For nucleus staining with Hoechst 33258 (Hoechst, Frankfurt, Germany), CGC were grown on a cover glass. After removing the medium, the neurons were washed two times with ice-cold PBS, fixed with 3% glutaraldehyde in PBS for 30 min at 4°, and washed again with PBS three times. Cells were then stained with Hoechst 33258 (0.4 μg/ml in PBS) for 15 min at 37°, washed, and mounted in 50% glycerol in PBS. Nuclei were visualized using a Olympus IMT-2 fluorescence microscope with a 60$\times$ magnification objective.

Synthesis of antisense and sense oligonucleotides. The phosphorothioate analogues of a 20-mer antisense and sense oligodeoxyribonucleotides to the rat GAPDH transcript were synthesized by using the sulfurizing reagent as previously described (15). Underlining indicates the phosphorothioated nucleotides. The GAPDH antisense-1 oligonucleotide sequence was 5′-GACCTTCACCATCTTGTCTA-3′, which corresponds to a sequence of the rat GAPDH gene (16) that flanks the ATG initiation codon. The GAPDH antisense-2 oligonucleotide sequence was 5′-GTGGATGCAGGGATGATGTT-3′, and its sequence corresponds to the nucleotide sequence between 637 and 656 of the coding region of rat GAPDH mRNA. The sequences of the sense-1 and sense-2 oligonucleotides were the exact inverse of their respective antisense oligonucleotides, with phosphorothioate bonds in the corresponding position. A concentration of 10 μM GAPDH antisense oligonucleotide was found to be optimal for the present antisense knock-down study. For comparative studies, antisense oligonucleotides to lactate dehydrogenase and protein kinase C2 were also constructed. The lactate dehydrogenase antisense oligonucleotide sequence corresponded to the flanking initiation codon of the mRNA of the mouse gene (i.e., 5′-GAGGGTTGCCATCTTGGACT-3′). The protein kinase C antisense oligonucleotide sequence was against the flanking termination codon of the mRNA of the human gene (i.e., 5′-GTTCTCGCTGGTGAGTTTCA-3′). The latter was phosphorothioated throughout sequence.

Northern blotting. Total RNA isolation and Northern blot analysis were performed essentially as described previously (17), except that the human GAPDH and/or β-actin cDNA probe were 1.1- and 1.8-kb in length, respectively (Clontech, Palo Alto, CA) and that high-stringency washing of the hybridized blots was performed in 0.1$\times$ standard saline citrate (1$\times$ = 150 mM NaCl, 15 mM sodium citrate) containing 0.1% SDS at 60° for 10 min (one or two times). Approximately 9 μg of total RNA from each sample was separated by electrophoresis through a 1.2% agarose-formaldehyde gel. GAPDH mRNA bands were then quantified by charge-coupled device densitometry of the autoradiograms. GAPDH and β-actin mRNA levels were normalized to total cellular RNA in each sample, as described previously (17).

SDS-PAGE and Western blot analyses. At the indicated length of exposure to low K^+ concentrations, cells were harvested from the dish and then sonicated in 50 mM Tris·HCl, pH 7.4. After centrifugation of the homogenate at 200,000 $\times$ g for 30 min, the particulate fraction (pellet) was dissolved in a small volume of SDS (2%)-containing sample buffer. An aliquot of the samples (10–12 μg protein) was loaded onto each lane of the gel (8–16% linear gradient) for SDS-PAGE analysis, as described by Laemmli (18). The separated protein bands on the gel were visualized by using staining with 0.1% Coomassie brilliant blue. Western blotting was performed after transferring proteins on the gel to a polyvinylidene difluoride membrane (Polyscreen; DuPont-New England Nuclear, Boston, MA) as described previously (10). For specific immunostaining of GAPDH protein, a mouse anti-rabbit GAPDH monoclonal antibody (Biogenesis, Poole, England) was used at the appropriate dilution in 0.5% skim milk, 20 mM Tris·HCl, pH 7.4, 137 mM NaCl, and 0.05% Tween 20 and allowed to react for 60 min at room temperature with the blotted membrane preincubated with 10% skim milk. Peroxidase-conjugated rabbit anti-mouse IgS antibody (Dako, Glostrup, Denmark) was used as a secondary antibody. The immunoreactive proteins were visualized by the enhanced chemiluminescence autography (Renaissance, DuPont-New England Nuclear). Chicken muscle GAPDH was a product of Sigma Chemical (St. Louis, MO). Quantification of a 38-kDa protein band on the gel and GAPDH protein band on the autogram was performed by using a charge-coupled device densitometric image analyzer.

Unless otherwise stated, results shown are from a typical experiment that was repeated three times with similar results.

Results

Characterization of low K^+-induced death of CGC. Switching culturing conditions of CGC at 7 DIV from medium containing high (25 mM) KCl concentrations to medium containing low (5 mM) KCl concentrations resulted in a time-dependent decrease in cell viability quantified by FDA/PI double staining (Fig. 1). The loss of neurons was approximately 51% at 24 hr and 77% at 48 hr. This low K^+-induced neuronal death was suppressed by CHX (5 μg/ml) and, to a lesser extent, by Act-D (1 μg/ml), whereas ATA (5 μM), a DNase inhibitor, was ineffective. Conversely, the continuous presence of 25 mM KCl after medium switch did not induce toxicity.

Light microscopic examination of CGC with FDA 24 hr after low K^+ exposure revealed a subpopulation of neurons that were swollen, round, and weakly labeled with FDA (Fig. 2B) compared with the unexposed CGC, which were devoid of these features (Fig. 2A). Electron microscopic examination of these swollen neurons showed morphological properties typical of necrotic injury [i.e., the presence of numerous vacuoles in the cytoplasm and disintegration of the inner mitochondrial membranes but no visible alteration of nuclear chromatin (Fig. 2C)].

By contrast, another population of CGC exposed to low K^+ for 24 hr showed morphological hallmarks of apoptosis revealed by ultrastructural changes and nuclear dye staining. Electron micrographs showed heterochromatic patches on the margin of the nuclear membrane and blebbing of the plasma membrane, which are characteristic of an early stage of apoptosis (Fig. 3B), as compared with the unexposed healthy cells (Fig. 3A). Typical hallmarks of a later stage of apoptosis were also observed. These included dense chromatin condensation (pyknosis), dilation of the endoplasmic reticulum, and intact mitochondrial structures (Fig. 3C). Investigation of the morphology of cells stained with a bisbenzimide dye (Hoechst 33258) also revealed a marked change in nuclear organization in some CGC during the course of low K^+-induced neuronal death. Twelve hours after low K^+ exposure (77.0% viability), some nuclear fragmenta-

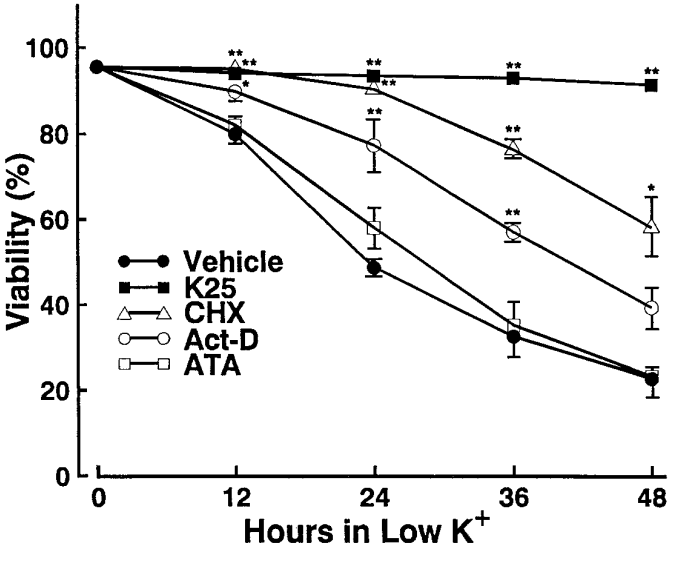

Fig. 1. Time course of the death of CGC exposed to low K^+. Neuroprotection by CHX, Act-D, or high KCl. CGC were prepared and cultured as described in Materials and Methods. At 7 DIV, the culture medium was replaced with a serum-free basal modified Eagle's medium containing 5 mM KCl with no additives (vehicle, i.e., H_2O), 25 mM KCl (*K25*), CHX (5 μg/ml), Act-D (1 μg/ml), or ATA (5 μM). At the indicated times after exposure to low K^+, neuronal viability was determined by FDA-PI double staining as described in Materials and Methods. Results are expressed as the mean ± standard error from three independent experiments. *, $p < 0.05$; **, $p < 0.01$ compared with the corresponding untreated (vehicle) control at each time using Student's *t* test.

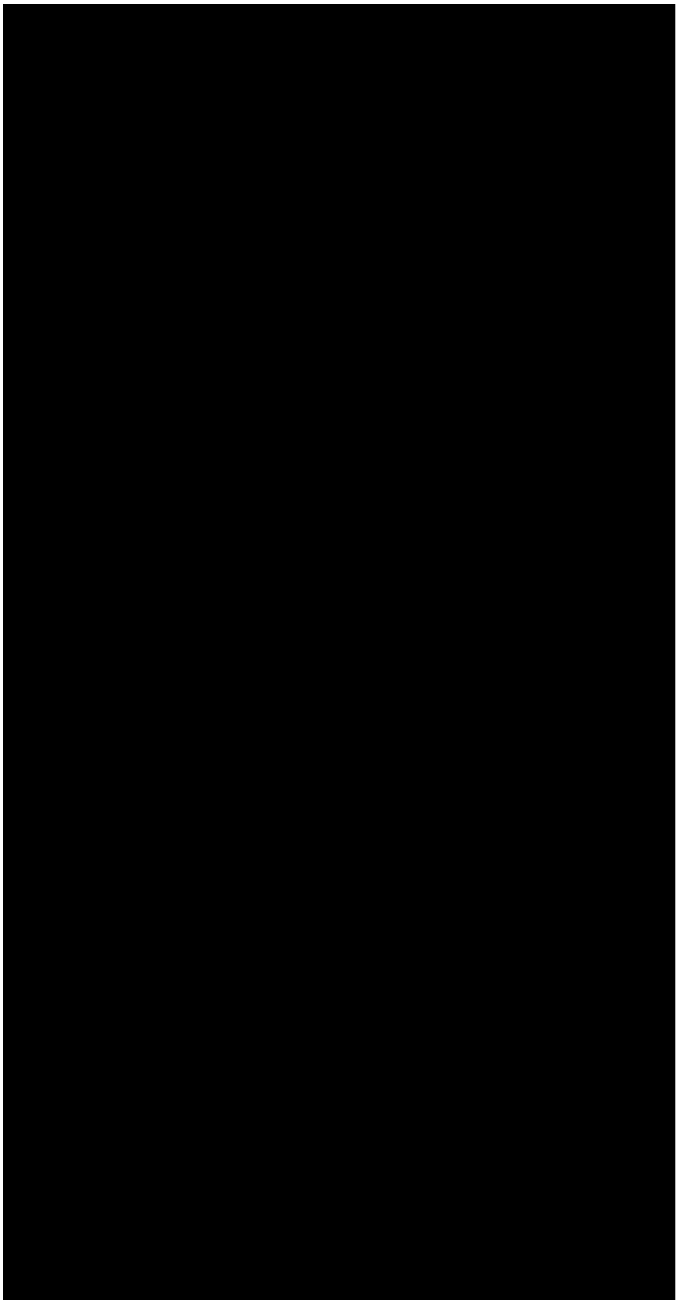

Fig. 2. Morphological features of CGC exposed to low K^+: FDA-PI fluorescence and electron microscopic examinations. At 24 hr after replacement with a serum-free medium containing 5 mM KCl, cultures were morphologically examined as described in Materials and Methods. Cells were stained with FDA and PI. A, Unexposed control. B, After 24-hr exposure to low K^+. Note that numerous swollen cells can be seen after low K^+exposure (*arrows*). *Scale bar*, 25 μm. C, A typical electron micrograph of the swollen cells shown in B. Note the high degree of vacuolization in the cytoplasm and damaged inner mitochondrial membranes (*arrowheads*). *Scale bar*, 1 μm.

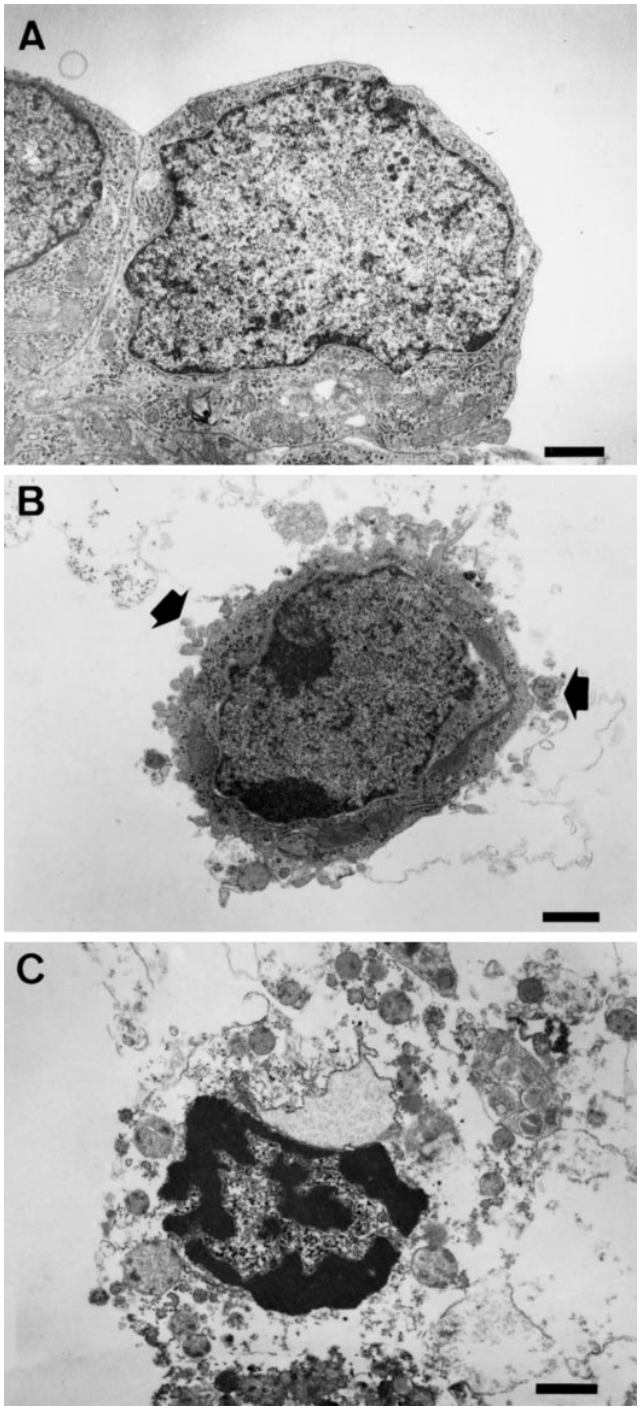

Fig. 3. Electron micrographs of CGC showing the morphological changes associated with apoptosis. CGC were exposed to low K^+ for 24 hr and then were subjected to electron microscopy as described in Materials and Methods. The viability of exposed cells was 53.2% at this point. A, Unexposed healthy cells. B, An early nuclear change during apoptosis. Heterochromatic patches were marginated at the nuclear membrane, and membrane-bound blebs (*arrows*) were found. C, A later stage of apoptotic death. The nucleus exhibited highly condensed chromatin, and a dilated, rough endoplasmic reticulum was observed. *Scale bar*, 1 μm.

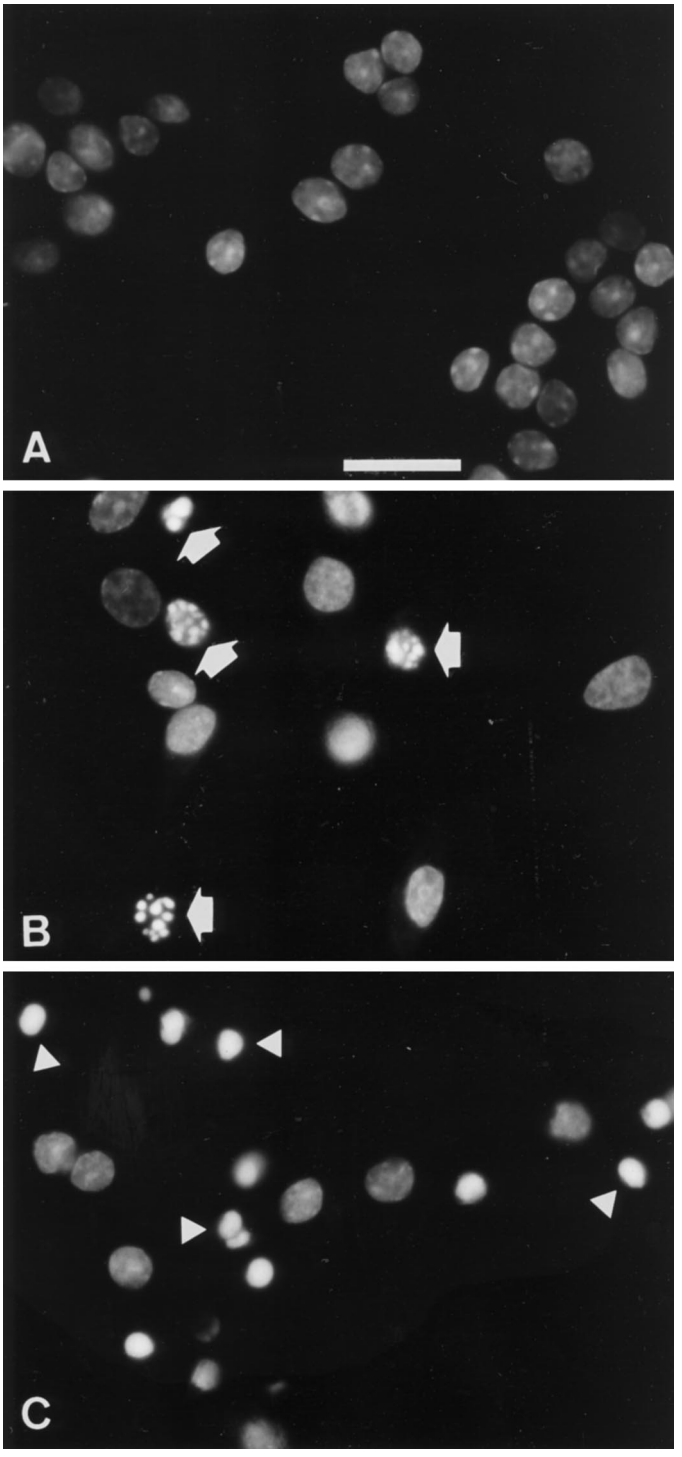

Fig. 4. Nuclear chromatin features of CGC exposed to low K^+. At 7 DIV, cultures were replaced with 5 mM KCl medium and, thereafter, at the indicated times, cells were fixed and stained using the DNA-specific fluorochrome Hoechst dye 33258 as outlined in Materials and Methods. A, Unexposed control. B, Twelve hours after exposure. C, Twenty-four hours after exposure. Note the typical features of apoptosis, namely, nuclear fragmentation (*arrows*) and chromatin condensation (*arrowheads*) in neurons in B and C. *Scale bar*, 20 μm.

tion was observed (Fig. 4B) compared with the unexposed control (Fig. 4A). At 24 hr (52.3% viability), the appearance of nuclei with condensed chromatin was more frequent (Fig. 4C). Additionally, we found a marked enhancement in internucleosomal DNA cleavage revealed by DNA ladders (multiples of 180 bp) on agarose gels after electrophoresis, which confirmed the previous reports of D'Mello *et al.* (7) (results not shown). Collectively, the above morphological results

strongly suggest that low K^+-induced death of CGC involved both apoptosis and necrosis. Careful morphological assessments and measurements of dead cells and intact nuclei (19) showed that, 24 hr after low K^+ exposure, approximately 70% of neurotoxicity was the result of apoptosis, and the remaining neurotoxicity was the result of necrosis.

Neuroprotective effects of GAPDH antisense oligodeoxyribonucleotides, CHX, and Act-D. The neuroprotective effects of RNA and protein synthesis inhibitors on low K^+-induced neuronal death suggest an involvement of *de novo* gene expression in this process. Because GAPDH overexpression has been linked to age-induced apoptosis of CGC (9, 10), we initially used the antisense knock-down strategy to examine the possible role of GAPDH in the neurotoxicity induced by low K^+ exposure. Both antisense-1 and antisense-2 oligodeoxyribonucleotides blocked low K^+-induced cell death at 24 hr by approximately 50%, whereas their corresponding sense oligonucleotides were ineffective (Fig. 5). As a negative control, we used two antisense oligonucleotides directed against lactate dehydrogenase and protein kinase C2. The former bears functional similarity to GAPDH, whereas the latter is abundantly expressed in CGC. Neither oligonucleotide showed a significant effect on low K^+-induced cell death. CHX almost completely blocked the death of CGC; however, Act-D was only as effective as the antisense oligonucleotides. Interestingly, an antidementia drug, THA (20), also showed weak but significant neuroprotection. In addition, MK-801, an antagonist of NMDA receptor, did not show any neuroprotective effect in the tested concentration range of 10^{-7} to 10^{-4} M (results not shown), which suggests that the low K^+-induced neurotoxicity was not the result of increased release of glutamate from CGC to act on NMDA receptors.

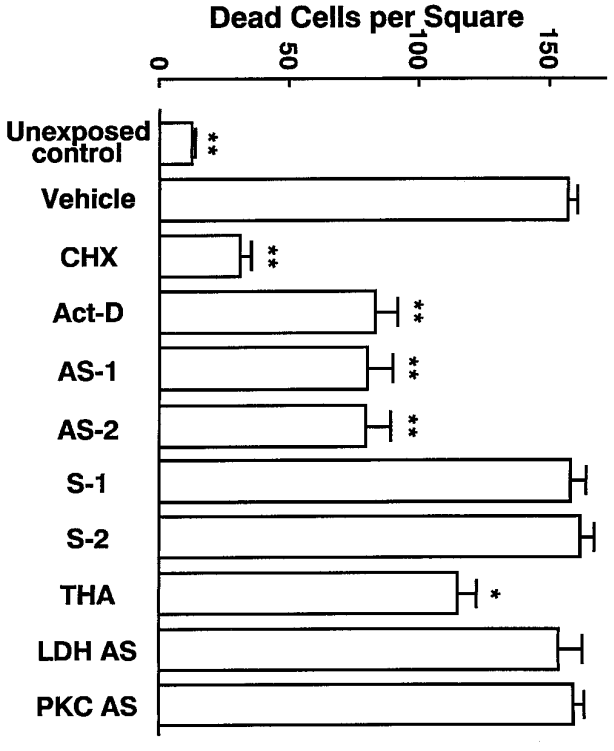

Fig. 5. Neuroprotective effects of GAPDH antisense oligonucleotides, Act-D, CHX, and THA on low K^+-induced neuronal death. CGC were exposed to low $K^+$and treated with indicated agents as described in the legend to Fig. 1, except that antisense or sense oligonucleotides (10 μM) and THA (50 μM) were also included in low K^+-exposed conditions. After 24-hr exposure to low K^+, the number of dead cells was assessed by using PI staining as described in Materials and Methods. *AS-1*, +GAPDH antisense-1 oligonucleotide; *AS-2*, +GAPDH antisense-2 oligonucleotide; *S-1*, +GAPDH sense-1 oligonucleotide; *S-2*, +GAPDH sense-2 oligonucleotide; *LDH AS*, +lactate dehydrogenase antisense oligonucleotide; *PKC AS*, +protein kinase C α antisense oligonucleotide. Values are the mean ± standard error of three independent experiments. *, $p < 0.01$; **, $p < 0.001$ compared with the untreated (vehicle) control using one-way analysis of variance followed with Dunnett's *t* test.

Direct visualization of living and dead cells by using double-labeled fluorescent microscopy revealed that, 24 hr after low K^+ exposure, the number of dead cells was markedly reduced by treatment with CHX, Act-D, or the antisense but not sense oligonucleotide (Fig. 6, A-D) compared with CGC exposed to low K^+ only (Fig. 2B). Importantly, the cell swelling associated with low K^+-induced neurotoxicity was abolished by CHX, whereas the antisense oligonucleotide and Act-D did not block the appearance of cell swelling. These results suggest that GAPDH and Act-D preferentially block apoptotic cell death with little or no effect on necrotic damage. Surprisingly, CHX seemed to block both apoptosis and necrotic injury of CGC.

Overexpression of GAPDH mRNA and protein levels: suppression by GAPDH antisense oligonucleotide, CHX, and Act-D. To demonstrate the validity of the antisense knock-down experiments, we studied the effects of the antisense oligonucleotide on GAPDH mRNA and protein levels. The level of GAPDH mRNA as measured by Northern blot hybridization increased 1 hr after low K^+ exposure, reaching a maximum at 2 hr, which was approximately 2.5-fold of the unexposed control (Fig. 7A). The level then declined at 3 hr and returned to the basal value at 4 hr. In contrast, the levels of β-actin mRNA remained relatively constant in the time course studied. The presence of the antisense but not sense oligonucleotide reduced the GAPDH mRNA to the control (Fig. 7B). CHX and Act-D also blocked the low K^+-induced GAPDH mRNA increase. CHX did not affect the viability and GAPDH mRNA level of CGC cultured in 25 mM K^+ (results not shown).

The high-speed particulate fraction of CGC homogenates was electrophoresed and stained on SDS-PAGE, and the amount of GAPDH (38-kDa band) was estimated. The level of the 38-kDa protein band was increased by approximately 2-fold 12 hr after low K^+-exposure (75.9% viability) (Fig. 8), and this increase was sustained at 24 hr. Treatment with GAPDH antisense but not its corresponding sense oligonucleotide completely blocked the increase in this protein, a result similar to the effect of CHX and/or Act-D. Although our previous microsequencing study showed that the bulk of this protein band on SDS-PAGE represented GAPDH protein (9), the reliability of the results obtained with SDS-PAGE analysis was further examined by means of Western blotting using a GAPDH-specific monoclonal antibody. As shown in Fig. 9, on the whole, Western blot analysis clearly confirmed the observations found using SDS-PAGE and shown in Fig. 8. The overexpressed GAPDH protein in the particulate fraction was suppressed by GAPDH antisense oligonucleotides in a concentration-dependent manner with an IC_{50} of approximately 2 μM (results not shown). Additionally, the level of GAPDH protein in the high-speed supernatant (cytosolic)

Fig. 6. Effects of GAPDH oligonucleotides, Act-D, and CHX on the morphology of CGC exposed to low K^+. Monolayered CGC cultures were treated with indicated agents as described in the legends to Figs. 1 and 5. Twenty-four hours after exposure to low K^+, cells were double-stained with FDA and PI and then photographed with a fluorescence microscope as described in Materials and Methods. A, CHX added. B, Act-D added. C, GAPDH antisense-1 oligonucleotide added. D, GAPDH sense-1 oligonucleotide added. Note that both the number of dead cells and the fragmentation of nerve fibers in D were effectively suppressed by CHX, Act-D, and the GAPDH antisense oligonucleotide; however, the swelling of neurons (*arrows*) was blocked only by CHX treatment as in A. The GAPDH sense-1 oligonucleotide did not show any neuroprotective effect; the experiment is thus similar to the vehicle control in Fig. 2B. *Scale bar*, 25 μm.

fraction was found to be unchanged during exposure of CGC to low K^+ (results not shown).

Discussion

In this study, we have characterized the neuronal damage of granule cells resulting from the switch of culturing conditions from high to low K^+ concentrations. We have confirmed previous reports that low K^+ culturing conditions induce apoptotic cell death (7, 8). Moreover, we have provided the first evidence that necrosis significantly contributes to this low K^+-induced neurotoxicity; e.g., morphological observations show that a subpopulation of neurons is swollen and shows extensive vacuolization in the cytoplasm and damaged mitochondria but no visible change in nuclear structures (Figs. 2 and 6). It was recently reported that NMDA or nitric oxide/superoxide can trigger either apoptotic or necrotic death of cultured cerebrocortical neurons depending on the intensity of the initial insults (21). The occurrence of both apoptosis and necrosis of CGC after a low K^+ concentration switch raises the possibility that these cultured neurons may not be homogeneous; a subpopulation of neurons may be more vulnerable than the others to necrotic insults. The heterogeneity of cultured CGC is also suggested by our receptor autoradiographic findings that a muscarinic receptor antagonist labels individual CGC unequally and that some CGC are not labeled at all (22).

In view of the involvement of GAPDH overexpression in age-induced apoptosis of CGC, we explored its role in low K^+-induced neuronal death. We found that both GAPDH antisense-1 (directed against the flanking region of the initiation site) and antisense-2 (directed against the coding region) oligonucleotides protect against low K^+-induced neuronal death by approximately 50% (Fig. 5). In contrast, two unrelated antisense oligonucleotides against lactate dehydrogenase and protein kinase C failed to provide protection (Fig. 5). Morphological inspection suggests that GAPDH antisense oligonucleotides preferentially protect against apoptosis with little or no effect on necrotic damage in CGC (Fig. 6). That the antisense protection is related to GAPDH knockdown is supported by the observations that the antisense but not sense oligonucleotides suppress the overexpressed GAPDH mRNA and protein levels (Figs. 7, 8, and 9). Low

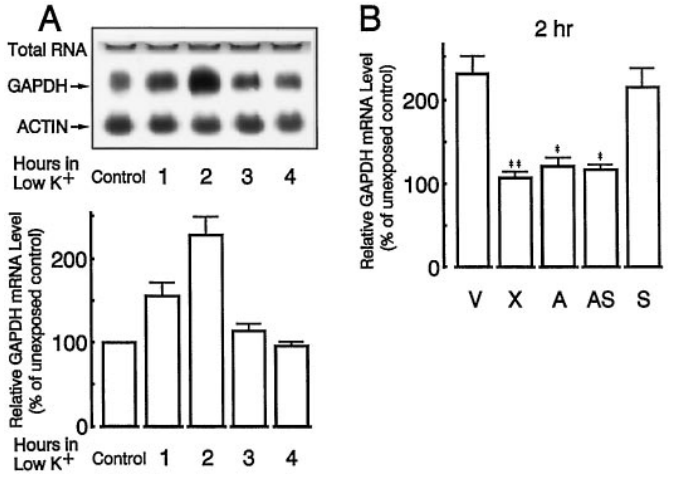

Fig. 7. Northern blot analysis of GAPDH mRNA levels in CGC during exposure to low K^+: time course and effects of GAPDH oligonucleotides, Act-D, and CHX. Mature CGC were treated with indicated agents as described in the legends to Figs. 1 and 5. Experimental conditions for the Northern analysis are as described in Materials and Methods. A fraction of each sample was used for the quantification of total RNA by densitometry of photographic negatives taken of ethidium bromide-stained agarose gel as described previously (17). *Bar graphs,* levels of quantified GAPDH mRNA are expressed as values relative to the unexposed control. A, Time course of changes in GAPDH mRNA levels in neurons after low K^+ exposure. Note the relatively constant level of β-actin mRNA (*ACTIN*). B, Effects of GAPDH oligonucleotides, Act-D, and CHX on the overexpressed GAPDH mRNA levels induced by low K^+ exposure for 2 hr. Values are the mean ± standard error of three independent experiments. *, $p < 0.01$; **, $p < 0.001$ compared with the untreated (vehicle) control using one-way analysis of variance followed with Dunnett's *t* test. *V*, vehicle; *X*, +CHX; *A*, +Act-D; *AS*, +GAPDH antisense-2 oligonucleotide; *S*, +GAPDH sense-2 oligonucleotide.

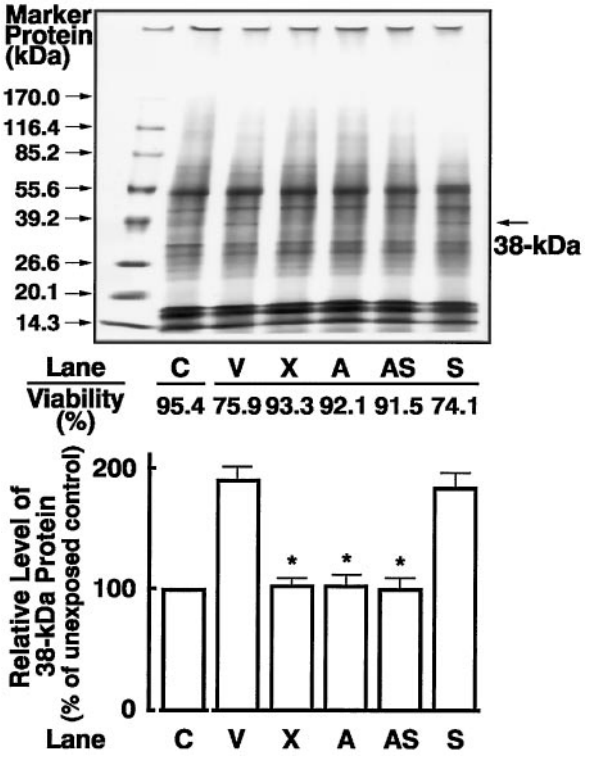

Fig. 8. SDS-PAGE analysis of particulate proteins of CGC: effects of GAPDH oligonucleotides, Act-D, and CHX. Cells were treated with indicated agents as described in the legends to Figs. 1 and 5 and then harvested at 12 hr after low K^+ exposure. Experimental conditions for SDS-PAGE analysis are as described in Materials and Methods. An aliquot of the samples was loaded onto each lane of the gel. *Left lane,* marker proteins for molecular mass (kDa). Measurements of cell viability and level of the 38-kDa protein are as described in Materials and Methods. *Bars,* Levels of quantified 38-kDa proteins expressed as relative values compared with the unexposed control (C). Values are the mean ± standard error of three independent experiments. *, $p < 0.001$ compared with the untreated (vehicle) control using one-way analysis of variance followed with Dunnett's *t* test. *V*, vehicle; *X*, +CHX; *A*, +Act-D; *AS*, +GAPDH antisense-1 oligonucleotide; *S*, +GAPDH sense-1 oligonucleotide.

K^+-induced GAPDH mRNA accumulation peaks 2 hr after medium switch (Fig. 7A). This GAPDH up-regulation is temporally related to the report by Galli *et al.* (23) in that the effective rescue of CGC exposed to low K^+ can occur only if Act-D is added before 2 hr after low K^+ exposure. The antisense protection does not seem to be the result of inhibition of global protein synthesis, because GAPDH antisense oligonucleotides did not significantly affect [^{3}H]leucine incorporation into proteins under our low K^+ experimental conditions (results not shown). Taken together, our results strongly suggest that, as in age-induced and cytosine arabinoside-induced apoptosis (9, 11, 12), GAPDH overexpression is also involved in low K^+-induced apoptosis but not necrosis of CGC.

Similar to the GAPDH antisense oligonucleotide, Act-D also partially blocks low K^+-induced death of CGC, and its protection is predominantly for the apoptotic rather than necrotic neurons (Figs. 5 and 6). Unexpectedly, CHX was found to inhibit both apoptotic and necrotic damage of CGC, producing the most robust protection (Figs. 5 and 6). These results seem to be paradoxical, inconsistent with the general rule that necrosis does not require *de novo* protein synthesis (for a review, see Ref. 24). Given that secondary necrosis has been proposed to be the result of a progression or extension of apoptosis in some cases, depending on mitochondrial function (25), it is not surprising that some parallels exist between apoptosis and necrosis and that there are certain genetically programmed responses to both types of stimuli. In this context, we found that the occurrence of swollen cells was apparent approximately 12 hr after low K^+ exposure, reached a maximum at 24 hr, and declined drastically between 36 and 48 hr (results not shown). It is of interest that the protective effects elicited by the antisense oligonucleotides, Act-D, and CHX are all associated with the suppression of low K^+-induced up-regulation of GAPDH mRNA and a selective blockade of the overexpressed GAPDH protein (Figs. 7, 8, and 9). In all cases, the basal, constitutive levels of GAPDH mRNA and protein were unaffected by these neuroprotectants. This suggests that there may be multiple pools of GAPDH mRNA and protein that are subjected to differential regulation. This notion is consistent with reports that there are more than 300 copies of GAPDH genes in the rat genome (16) and that GAPDH protein is located in multiple cellular compartments, including the plasma membrane, mitochondria, cytoskeletons, and nuclei (26, 27). Low K^+-induced cell death is also significantly protected by the antidementia drug, THA, but not by the endonuclease inhibitor, ATA, at 5 μM (Figs. 1 and 5). Regarding the neuroprotective effect of THA, it is intriguing to note that a monoclonal antibody raised against amyloid plaques from Alzheimer's patients' brains reacts with both the overexpressed 38-kDa protein (i.e., GAPDH) and the β-amyloid precursor protein

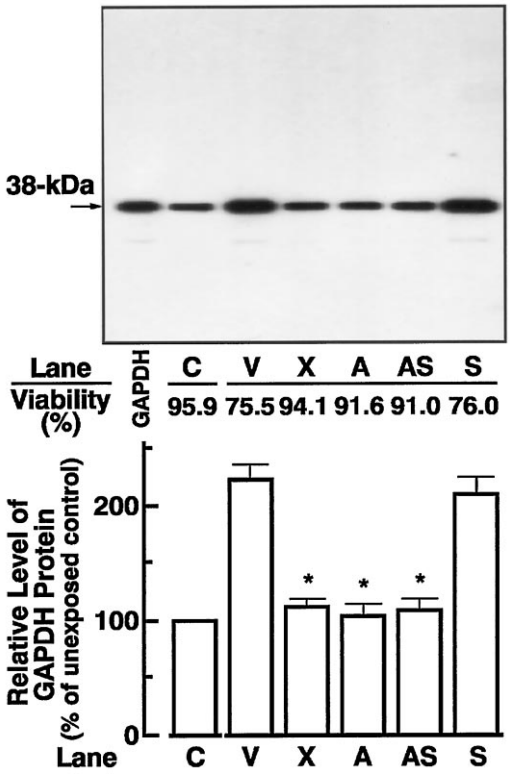

Fig. 9. Immunoblotting patterns of CGC particulate proteins and purified GAPDH. Various particulate fractions derived from CGC at 12 hr after low K^+ exposure were subjected to SDS-PAGE for Western blotting as illustrated in Fig. 8. After protein transfer, the blot was incubated with GAPDH monoclonal antibody as described in Materials and Methods. Measurements of cell viability and level of GAPDH protein on the autogram are also described in Methods. *Bar graph,* levels of quantified GAPDH proteins. These results are expressed as relative values compared with the unexposed control (C). Values are the mean ± standard error of three independent experiments. *, $p < 0.001$ compared with the untreated (vehicle) control using one-way analysis of variance followed with Dunnett's *t* test. *V*, vehicle; *X*, +CHX; *A*, +Act-D; *AS*, +GAPDH antisense-1 oligonucleotide; *S*, +GAPDH sense-1 oligonucleotide. Note that a very low level of a low-molecular-mass protein present in *V* and *S* is also immunoreactive; this protein can be seen in the purified GAPDH preparation.

(10), which supports a previous report that GAPDH interacts with the β-amyloid precursor protein (28). Higher concentrations of ATA (10–50 μM) exacerbate the cell death (results not shown), which suggests that CGC exposed to low K^+ are vulnerable to this insult. The ATA neurotoxicity could be related to its diversity of actions, including inhibition of NMDA receptor function, nucleic acid polymerase activity, or protein synthesis (29–31).

The mechanisms underlying GAPDH overexpression in CGC exposed to low K^+ are unclear, but the induction is likely to be triggered by lowering the intracellular Ca^{2+} level. In a related study using cultured sympathetic neurons, it has been shown that programmed cell death triggered by nerve growth factor withdrawal is effectively suppressed by thapsigargin-induced Ca^{2+} influx (32) and is associated with the expression of various protooncogenes (33). It remains to be studied whether these protooncogenes are also induced in CGC exposed to low K^+ and, if so, whether these induced protooncogenes serve as transcriptional factors in mediating the expression of GAPDH. GAPDH is an enzyme with multiple functions and is present not only in the cytosolic but also in the particulate fraction. The present and previous studies (9, 12) show that the overexpressed GAPDH protein is located in the particulate fraction where most of the nonglycolytic activities of GAPDH are found. Thus, some of these nonglycolytic functions may play a role in neuronal apoptosis. These include bundling of microtubules (34), binding to β-amyloid precursor protein (28), modulation of actin-filament network (35), facilitation of membrane fusion (36), and regulation of nuclear transcription and uracil DNA glycosylase activity (37, 38) as well as being the target of covalent NAD^+-linkage mediated by nitric oxide and oxygen free radicals (39, 40). Studies are in progress to determine which of these activities of the GAPDH protein are involved in the apoptosis of CGC.

References

1. Altman, J. Postnatal development of the cerebellar cortex in the rat. *J. Comp. Neurol.* **145:**353–398 (1972).
2. Burgoyne, R. D., and M. A. Cambray-Deakin. The cellular neurobiology of neuronal development: the cerebellar granule cell. *Brain Res. Rev.* **13:**77–101 (1988).
3. Wood, K. A., B. Dipasquale, and R. J. Youle. In situ labeling of granule cells for apoptosis-associated DNA fragmentation reveals different mechanisms of cell loss in developing cerebellum. *Neuron* **11:**621–632 (1993).
4. Wood, K. A., and R. J. Youle. The role of free radicals and p53 in neuron apoptosis *in vivo*. *J. Neurosci.* **15:**5851–5857 (1995).
5. Gallo, V., A. Kingsbury, R. Balázs, and O. S. Jørgensen. The role of depolarization in the survival and differentiation of cerebellar granule cells in culture. *J. Neurosci.* **7:**2203–2213 (1987).
6. Balázs, R., O. S. Jørgensen, and N. Hack. *N*-Methyl-D-aspartate promotes the survival of cerebellar granule cells in culture. *Neuroscience* **27:**437–451 (1988).
7. D'Mello, S. R., C. Galli, T. Ciotti, and P. Calissano. Induction of apoptosis in cerebellar granule neurons by low potassium: inhibition of death by insulin-like growth factor I and cAMP. *Proc. Natl. Acad. Sci. USA* **90:**10989–10993 (1993).
8. Yan, G.-M., B. Ni, M. Weller, K. A. Wood, and S. M. Paul. Depolarization or glutamate receptor activation blocks apoptotic cell death of cultured cerebellar granule neurons. *Brain Res.* **656:**43–51 (1994).
9. Ishitani, R., K. Sunaga, A. Hirano, P. Saunders, N. Katsube, and D.-M. Chuang. Evidence that glyceraldehyde-3-phosphate dehydrogenase is involved in age-induced apoptosis in mature cerebellar neurons in culture. *J. Neurochem.* **66:**928–935 (1996).
10. Sunaga, K., H. Takahashi, D.-M. Chuang, and R. Ishitani. Glyceraldehyde-3-phosphate dehydrogenase is over-expressed during apoptotic death of neuronal cultures and is recognized by a monoclonal antibody against amyloid plaques from Alzheimer's brain. *Neurosci. Lett.* **200:**133–136 (1995).
11. Ishitani, R., M. Kimura, K. Sunaga, N. Katsube, M. Tanaka, and D.-M. Chuang. An antisense oligodeoxynucleotide to glyceraldehyde-3-phosphate dehydrogenase blocks age-induced apoptosis of mature cerebrocortical neurons in culture. *J. Pharmacol. Exp. Ther.* **278:**447–454 (1996).
12. Ishitani, R., and D.-M. Chuang. Glyceraldehyde-3-phosphate dehydrogenase antisense oligodeoxynucleotides protect against cytosine arabinonucleoside-induced apoptosis in cultured cerebellar neurons. *Proc. Natl. Acad. Sci. USA* **93:**9937–9941 (1996).
13. Sunaga, K., M. Tanaka, H. Aishita, D.-M. Chuang, and R. Ishitani. Glyceraldehyde-3-phosphate dehydrogenase (GAPDH) antisense oligodeoxynucleotide protects against low K^+-induced apoptosis of cultured cerebellar neurons. *Soc. Neurosci. Abstr.* **21:**1554 (1995).
14. Jones, K. H., and J. A. Senft. An improved method to determine cell viability by simultaneous staining with fluorescein diacetate-propidium iodide. *J. Histochem. Cytochem.* **33:**77–79 (1985).
15. Iyer, R. P., W. Egan, J. B. Regan, and S. L. Beaucage. 3*H*-1,2-Benzodithiol-3-one 1,1-dioxide as an improved sulfurizing reagent in the solid-phase synthesis of oligodeoxyribonucleoside phosphorothioates. *J. Am. Chem. Soc.* **112:**1253–1254 (1990).
16. Tso, J. Y., X.-H. Sun, T.-H. Kao, K. S. Reece, and R. Wu. Isolation and characterization of rat and human glyceraldehyde-3-phosphate dehydrogenase cDNAs: genomic complexity and molecular evolution of the gene+. *Nucleic Acids Res.* **13:**2485–2502 (1985).
17. Fukamauchi, F., C. Hough, and D.-M. Chuang. Expression and agonist-induced down-regulation of mRNAs of m2- and m3-muscarinic acetylcholine receptors in cultured cerebellar granule cells. *J. Neurochem.* **56:**716–719 (1991).
18. Laemmli, U. K. Cleavage of structural proteins during the assembly of the head of bacteriophage T4. *Nature (Lond.)* **227:**680–685 (1970).
19. Sunaga, K., D.-M. Chuang, and R. Ishitani. Tetrahydroaminoacridine is neurotrophic and promotes the expression of muscarinic receptor-coupled

phosphoinositide turnover in differentiating cerebellar granule cells. *J. Pharmacol. Exp. Ther.* **264:**463–468 (1993).
20. Summers, W. K., L. V. Majovski, G. M. Marsh, K. Tachiki, and A. Kling. Oral tetrahydroaminoacridine in long-term treatment of senile dementia, Alzheimer type. *N. Engl. J. Med.* **315:**1241–1245 (1986).
21. Bonfoco, E., D. Krainc, M. Ankarcrona, P. Nicotera, and S. A. Lipton. Apoptosis and necrosis: two distinct events induced, respectively, by mild and intense insults with *N*-methyl-D-aspartate or nitric oxide/superoxide in cortical cell cultures. *Proc. Natl. Acad. Sci. USA* **92:**7162–7166 (1995).
22. Sunaga, K., D.-M. Chuang, and R. Ishitani. Autoradiographic demonstration of an increase in muscarinic cholinergic receptors in cerebellar granule cells treated with tetrahydroaminoacridine. *Neurosci. Lett.* **151:**45–47 (1993).
23. Galli, C., O. Meucci, A. Scorziello, T. M. Werge, P. Calissano, and G. Schettni. Apoptosis in cerebellar granule cells is blocked by high KCl, forskolin, and IGF-1 through distinct mechanisms of action: the involvement of intracellular calcium and RNA synthesis. *J. Neurosci.* **15:**1172–1179 (1995).
24. Margolis, R. L., D.-M. Chuang, and R. M. Post. Programmed cell death: implications for neuropsychiatric disorders. *Biol. Psychiatry* **35:**946–956 (1994).
25. Ankarcrona, M., J. M. Dypbukt, E. Bonfoco, B. Zhivotovsky, S. Orrenius, S. A. Lipton, and P. Nicotera. Glutamate-induced neuronal death: a succession of necrosis or apoptosis depending on mitochondrial function. *Neuron* **15:**961–973 (1995).
26. Rogalski, A. A., T. L. Steck, and A. Waseem. Association of glyceraldehyde-3-phosphate dehydrogenase with the plasma membrane of the intact human red blood cell. *J. Biol. Chem.* **264:**6438–6446 (1989).
27. Singh, R., and M. R. Green. Sequence-specific binding of transfer RNA by glyceraldehyde-3-phosphate dehydrogenase. *Science (Washington D. C.)* **259:**365–368 (1993).
28. Schulze, H., A. Schuler, D. Stüber, H. Döbeli, H. Langen, and G. Huber. Rat brain glyceraldehyde-3-phosphate dehydrogenase interacts with the recombinant cytoplasmic domain of Alzheimer's β-amyloid precursor protein. *J. Neurochem.* **60:**1915–1922 (1993).
29. Zeevalk, G. D., D. Schoepp, and W. J. Nicklas. Aurintricarboxylic acid prevents NMDA-mediated excitotoxicity: evidence for its action as an NMDA receptor antagonist. *J. Neurochem.* **61:**386–389 (1993).
30. Givens, J. F., and K. F. Manly. Inhibition of RNA-directed DNA polymerase by aurintricarboxylic acid. *Nucleic Acids Res.* **3:**405–418 (1976).
31. Grollman, A. P., and M. L. Stewart. Inhibition of the attachment of messenger ribonucleic acid to ribosomes. *Proc. Natl. Acad. Sci. USA* **61:**719–725 (1968).
32. Lampe, P. A., E. B. Cornbrooks, A. Juhasz, E. M. Johnson, Jr., and J. L. Franklin. Suppression of programmed neuronal death by a thapsigargin-induced Ca^{2+} influx. *J. Neurobiol.* **26:**205–212 (1995).
33. Estus, S., W. J. Zaks, R. S. Freeman, M. Gruda, R. Bravo, and E. M. Johnson, Jr. Altered gene expression in neurons during programmed cell death: identification of c-*jun* as necessary for neuronal apoptosis. *J. Cell Biol.* **127:**1717–1727 (1994).
34. Huitorel, P., and D. Pantaloni. Bundling of microtubules by glyceraldehyde-3-phosphate dehydrogenase and its modulation by ATP. *Eur. J. Biochem.* **150:**265–269 (1985).
35. Füchtbauer, A., B. M. Jockusch, E. Leberer, and D. Pette. Actin-severing activity copurifies with phosphofructokinase. *Proc. Natl. Acad. Sci. USA* **83:**9502–9506 (1986).
36. Glaser, P. E., and R. W. Gross. Rapid plasmenylethanolamine-selective fusion of membrane bilayers catalyzed by an isoform of glyceraldehyde-3-phosphate dehydrogenase: discrimination between glycolytic and fusogenic roles of individual isoforms. *Biochemistry* **34:**12193–12203 (1995).
37. Morgenegg, G., G. C. Winkler, U. Hübscher, C. W. Heizmann, J. Mous, and C. C. Kuenzle. Gylceraldehyde-3-phosphate dehydrogenase is a nonhistone protein and a possible activator of transcription in neurons. *J. Neurochem.* **47:**54–62 (1986).
38. Meyer-Siegler, K., D. J. Mauro, G. Seal, J. Wurzer, J. K. DeRiel, and M. A. Sirover. A human nuclear uracil DNA glycosylase is the 37-kDa subunit of glyceraldehyde-3-phosphate dehydrogenase. *Proc. Natl. Acad. Sci. USA* **88:**8460–8464 (1991).
39. McDonald, L. J., and J. Moss. Stimulation by nitric oxide of an NAD linkage to glyceraldehyde-3-phosphate dehydrogenase. *Proc. Natl. Acad. Sci. USA* **90:**6238–6241 (1993).
40. Marin, P., M. Maus, J. Bockaert, J. Glowinski, and J. Prémont. Oxygen free radicals enhance the nitric oxide-induced covalent NAD^+-linkage to neuronal glyceraldehyde-3-phosphate dehydrogenase. *Biochem. J.* **309:**891–898 (1995).

Send reprint requests to: Ryoichi Ishitani, Ph.D., Group on Cellular Neurobiology, Josai University, Sakado, Saitama 350–02, Japan